Chapter 5

A Multiplexed, Two-Electrode Platform for Biosensing based on DNA-Mediated Charge Transport

Adapted from: Furst, A. L., Hill, M. G., and Barton, J. K. (2015) A Multiplexed, Two-Electrode Platform for Biosensing based on DNA-Mediated Charge Transport, *Submitted.*

Introduction

Analytical methods for reliable biomolecule detection are becoming increasingly important with the continued discovery of disease-related biomarkers. Electrochemical nucleic acid-based assays,[1-10] particularly those that utilize DNA-mediated charge transport (DNA CT)[11, 12] are especially promising for sensing platforms. Devices based on DNA CT effectively report on the integrity of the π-stacked DNA bases; perturbations to the proper stacking, resulting from lesions, single nucleotide polymorphisms, or protein binding events that affect the base stack, attenuate the electrochemical signal. DNA CT has been employed successfully in the detection of a variety of biomolecules, including DNA fragments, chemically modified DNA, and DNA-binding proteins, many of which are not specifically detectable using alternative sensing platforms.[11, 13]

Substrates for DNA-based electrochemical systems typically are prepared by self-assembling thiolated DNA duplexes onto gold electrodes, followed by backfilling with an alkylthiol to passivate any remaining surface-exposed gold.[14-16] One major challenge with this methodology is the limited control over monolayer composition, both in the total amount of DNA assembled and its dispersion within the monolayer.[17-19] For biosensing applications, which rely on direct interactions between target biomolecules and the DNA duplexes attached to the electrode surface, homogeneous spacing between the DNA duplexes is critical to provide the target in solution adequate access to individual helices. Inevitably, clustering occurs with thiolated DNA. Recently, we demonstrated the utility of applying mixed alkylthiol monolayers doped with variable amounts of azide-terminated functional groups to gain more control over monolayer formation.[20] These monolayers are significantly more homogeneous than those prepared

using thiolated DNA. Additionally, coupling with copper-free click conjugation of cyclooctyne-labeled DNA yields surfaces containing evenly dispersed rather than clustered DNA with coverages that mirror the mole fraction of azide in the underlying film. The resulting monolayers allow greater access of DNA-binding proteins to individual helices within the films, permitting devices with greater sensitivity to these biomolecules.

While tethering DNA to surfaces with cyclooctynes provides a strong foundation for more controlled monolayer formation, ideally, DNA probe molecules would feature a simple terminal alkyne group to avoid additional synthetic steps. The well known Huisgen 1,3-dipolar cycloaddition ("click" reaction),[21] catalyzed by copper(I), has been used previously to form homogenous monolayers with terminal alkyne-labeled probe molecules.[22, 23] Indeed, because of the instability of copper(I) in aqueous solution and its reactivity with DNA,[24-26] electrochemical methods to generate copper(I) *in situ* from copper(II) precursors have been developed, and the coupling of alkyne-labeled oligonucleotides to azide-terminated surfaces *via* electrochemically induced click chemistry has been reported.[27-30]

We have now employed a multiplexed platform in which simple alkyne-labeled duplexes are coupled to azide-terminated surfaces by copper(I) species generated electrochemically *in situ* at a secondary working electrode positioned over the alkylthiol monolayer.[31] Our attempts to fabricate surfaces suitable for DNA CT using published methods with one working electrode were difficult: reliable electrochemical readout of DNA-mediated chemistry was hampered by interference from the irreversible products of copper(II) reduction at the modified electrochemical surface (likely adsorption of copper

films onto the electrode surface). Our new method[31] allows for the attachment of multiple DNA sequences onto a single electrode, with tight control over the probe-molecule spacing.[32] A multiplexed version of this methodology has enabled the sensitive detection of DNA methyltransferase activity directly from human tissue samples.[33]

Here we report the full characterization of this multiplexed, two working electrode platform that enables both catalyst activation and electrochemical readout from a secondary electrode. In addition to minimizing undesirable copper products at DNA-modified surfaces, we have found that readout of electrocatalytically generated reporter molecules at the secondary electrode greatly enhances the sensitivity and specificity of DNA CT assays. We have optimized the spacing between the primary and secondary electrodes such that we are no longer limited by the diffusion of the electrocatalytic components, and this mode of detection importantly eliminates large background signals. Indeed, this platform enables detection of single base mismatches as well as the selective and specific detection of two transcription factors, TATA binding protein (TBP) and CopG, with sensitivities greater than those achieved with single working electrode platforms.

Materials and Methods

Preparation of Surfaces and First Alkanethiol Monolayers

Gold surfaces were polished with 0.05 μm alumina slurries (Buhler) before monolayer assembly. Mixed monolayers were then formed on the substrate plate by self-assembly of 100 mM 12-azidododecane-1-thiol (C_{12} thiol azide) and 100 mM 11-mercaptoundecyl-phosphoric acid from an ethanolic solution. Surfaces were incubated in the thiol solution for 18-24 h, followed by rinsing with ethanol and phosphate buffer (5 mM phosphate, 50 mM NaCl, pH 7.0).

DNA Synthesis and Purification

Hexynyl-labeled oligonucleotides were synthesized on an Applied Biosystems 3400 DNA synthesizer, and were modified at the 5` end with a C6-alkyne reagent purchased from Glen Research, Inc. Complementary unmodified strands were purchased from IDT. DNA strands modified with Nile Blue at the 5` terminus were prepared as previously reported.[34] Briefly, DNA was synthesized with ultramild reagents (Glen Research, Inc) to prevent Nile Blue degradation, and 5-[3-acrylate NHS ester]-deoxy uridine was incorporated as the 5` terminal base. With DNA on the solid support, 10 mg/mL Nile Blue perchlorate in 9:1 *N,N*-dimethylformamide/*N,N*-diisopropylethylamine (Sigma Aldrich) was added and allowed to shake for 24 h. Beads were washed three times each with *N,N*-dimethylformamide, methanol, and acetonitrile. The DNA was removed from the solid support with 0.05 M potassium carbonate in methanol at ambient temperature for 24 h. Preparation of all oligonucleotides followed a reported protocol. For non-ultramild syntheses, DNA was deprotected and cleaved from the solid support

with ammonium hydroxide (60° C for 12 h). Following a preliminary round of high-performance liquid chromatography (HPLC) on a PLRP-S column (Agilent), oligonucleotides were treated with 80% acetic acid in water for 20 minutes. Each oligonucleotide was again purified by HPLC using a gradient of acetonitrile and 50 mM ammonium acetate. Oligonucleotides were then desalted by ethanol precipitation and quantified by ultraviolet-visible spectrophotometry based on their extinction coefficients at 260 nm (IDT Oligo Analyzer). Oligonucleotide masses were verified by matrix-assisted laser desorption (MALDI) mass spectrometry. DNA duplexes were formed by thermally annealing equimolar amounts of single-stranded oligonucleotides in deoxygenated phosphate buffer (5mM phosphate, 50 mM NaCl, pH 7.0) at 90° C for 5 minutes followed by slowly cooling to 25° C.

The following sequences were prepared:

Well Matched
Alkyne: H-C_2-$(CH_3)_6$-5'-GCT CAG TAC GAC GTC GA-3'
Complement: 3'-CGA GTC ATG CTG CAG CT-5'

Mismatched
Alkyne: H-C_2-$(CH_3)_6$-5'-GCT CAG TA*C* GAC GTC GA-3'
Complement: 3'-CGA GTC AT*A* CTG CAG CT-5'

TBP Binding Sequence
Alkyne: H-C_2-$(CH_3)_6$-5'-GGC GTC **TAT A**AA GCG ATC GCG A-3'
Complement: 3'-CCG CAG **ATA T**TT CGC TAC CGC T-5'

COPG Binding Sequence
Alkyne: H-C_2-$(CH_3)_6$-5'-AAC CG**T GCA** CTC AA**T GCA** ATC-3'
Complement: 3'-TTG GC**A CGT** GAG TT**A CGT** TAG-5'

The location of the mismatch is indicated in italics and with an underline, and the protein binding sites are shown in bold.

Design of Experimental Platform

The multiplexed, two-electrode array consisted of two ¼" Teflon blocks separated by a Teflon gasket of various thicknesses (Figure 5.1). Gold wires (1-mm diameter) were then inserted into holes drilled into the Teflon blocks to form complementary 5 x 3 electrode arrays on each block. Each pair of complementary electrodes was 5 mm from its nearest neighbor, providing the opportunity to isolate each pair into individual wells. The electrodes were sealed into the Teflon using superglue. The top array featured additional holes (1.5-mm diameter) to provide the reference and auxiliary electrodes access to the working solution. Spacers that separated the individual wells were constructed from 1.5 mm thick Teflon.

DNA Attachment to Alkanethiol Monolayers

A 10 mM aqueous $[Cu(phendione)_2]^{2+}$ (phendione=1,10-phenanthroline-5,6-dione solution was prepared by combining one equivalent of $CuSO_4$ (10 μmol, 15.9 mg) with two equivalents of phendione (20 μmol, 42.0 mg) in 10 mL of deionized H_2O. ESI-MS: 580.2 (calc: 580.0). The complex was additionally isolated as the PF_6^- salt. Prior to application to the electrode surface, the complex was diluted to a final concentration of 1 mM in Tris buffer (10 mM Tris, 100 mM KCl, 2.5 mM $MgCl_2$, 1 mM $CaCl_2$, pH 7.6). The catalyst solution was combined with 5`-labeled ethynyl DNA (final concentration of 25 μM), and a constant potential of -350 mV v. AgCl/Ag was applied to the sensing (top) electrode array to reduce the Cu(II) and initiate the coupling of the DNA to the azide-terminated monolayers. The potential was applied for 15 minutes. Multiple sequences of DNA were attached to the array through the sequential activation of different secondary

electrodes. For example, well matched and mismatched DNA were attached to the same array through the preliminary activation of secondary electrodes one through nine in the presence of well matched DNA, followed by rinsing of the platform and subsequent activation of secondary electrodes ten through fifteen in the presence of DNA containing a single-base mismatch.

Characterization of DNA-modified Monolayers

All electrochemical experiments were performed on a CHInstruments 760E bipotentiostat. For electrochemical impedance spectroscopy experiments, 400 μM potassium ferricyanide in phosphate buffer (5 mM phosphate, 50 mM NaCl, pH 7.0) was used. For all other experiments, electrochemistry was conducted in Tris buffer (10 mM Tris, 100 mM KCl, 2.5 mM $MgCl_2$, 1 mM $CaCl_2$, pH 7.6) with 4 μM methylene blue and 300 μM potassium ferricyanide; for experiments with covalent Nile Blue, methylene blue was omitted. For mismatch discrimination and protein binding experiments, constant potential amperometry was used, with potential applied for 90 s. The primary electrode was held at -400 mV v. AgCl/Ag, and the secondary electrode was held at 350 mV v. AgCl/Ag. A Pt wire was incorporated as a counter electrode.

TBP and CopG Experiments

TATA-Binding Protein (TBP) was purchased from ProteinOne, and CopG was purchased from Origene. Both proteins were stored at -80° C until use. MicroBiospin 6 columns (BioRad) were used to exchange the shipping buffer for Tris buffer (10 mM Tris, 100 mM KCl, 2.5 mM $MgCl_2$, 1 mM $CaCl_2$, pH 7.6). Prior to electrochemical

measurements with CopG and TBP, electrodes were incubated with 1 μM Bovine serum albumin (BSA) for 30 min, followed by rinsing with Tris buffer (10 mM Tris, 100 mM KCl, 2.5 mM $MgCl_2$, 1 mM $CaCl_2$, pH 7.6). Protein solutions (4 μL) were added to each electrode and incubated for 20 minutes at ambient temperature prior to measurement.

Results and Discussion

We have designed and fabricated an addressable, multiplexed biosensing array that features two sets of complementary electrodes separated by a thin film (Figure 5.1). The bottom electrodes, which compose the primary array, are modified with covalently bound DNA sequences dispersed within a mixed alkylthiol monolayer, while the top electrodes, which form the secondary array, are unmodified and are used both for activating a DNA-coupling catalyst and for the electrochemical readout.

Electrochemical Response of Coupling Catalyst

The electrode platform, electrocatalytic detection scheme, and coupling reaction are shown in Figure 5.1. The electrochemical initiation of azide/alkyne coupling via Cu(II) reduction has been explored previously.[35] While several chelating ligands for copper(I) click chemistry have been reported, our experiments have focused on the bipyridyl derivative 1,10-phenanthroline-5,6-dione (phendione), as this ligand is commercially available and yields a water-soluble complex. The cyclic voltammogram (CV) of $[Cu(phendione)_2][SO_4]$ in Tris buffer shows several copper-centered reductions between + 0.20 and -0.40 V *vs.* AgCl/Ag (Figure 5.2). Importantly, these processes are only partially chemically reversible. The CV also shows a coupled oxidative response with a shape characteristic of anodic stripping, suggesting that the electrochemical reactions result in the adsorption of at least some copper-containing species onto the electrode surface. The deposition of copper following electrochemical reduction is further

supported by the formation of a visible, black surface film following the application of potentials in the range of -0.30 to -0.40 V *vs.* AgCl/Ag.

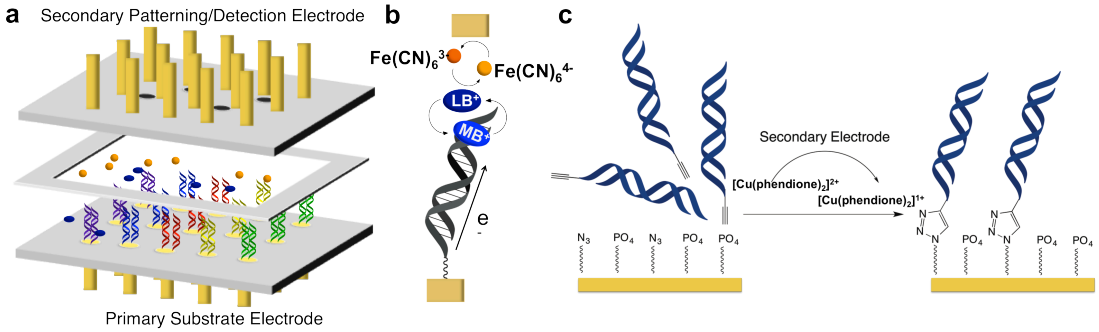

Figure 5.1 Multiplexed, two-electrode platform. a. The multiplexed platform contains two 5 x 3 arrays of 1 mm x 1.5 cm gold electrodes embedded in Teflon separated by a Teflon spacer to form a well for running solution. The secondary array (top) contains four holes into which reference and auxiliary electrodes can be inserted. A primary electrode array (bottom) forms the primary surface, and contains the same number and positioning of electrodes as the top array without holes. b. Electrocatalytic signal amplification occurs when a redox probe (blue oval) that interacts with the base stack of DNA is reduced *via* DNA-mediated CT. The probe then reduces an electron sink (orange ball) in solution, becoming reoxidized in the process. The reduced electron sink interacts with the secondary electrode, generating a current as it is reoxidized at the secondary electrode surface. c. DNA is covalently tethered to azide-containing monolayers on the substrate array by electrochemically activated click chemistry. A mixed monolayer containing azide head groups and phosphate head groups is formed on a gold surface. A solution of alkyne-modified DNA and the inert $[Cu(phendione)_2]^{2+}$ complex are added to the surface. Upon application of a sufficiently negative potential from the secondary electrode, the copper is reduced, yielding an active catalyst to covalently tether DNA to the mixed monolayer.

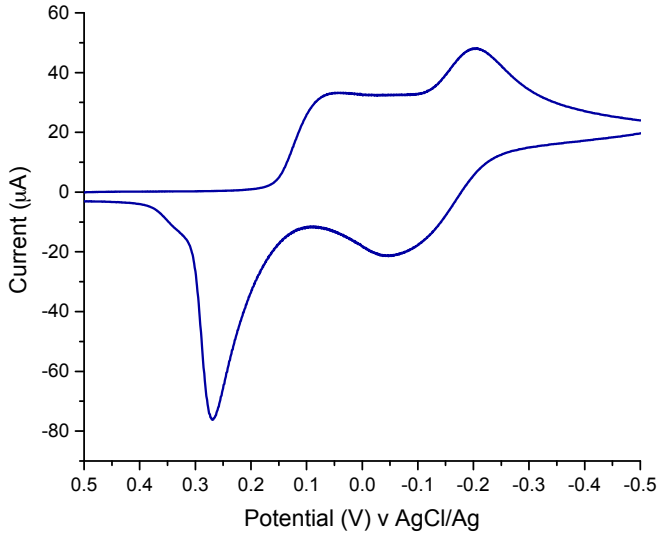

Figure 5.2 Electrochemistry of $[Cu(phendione)_2]^{2+}$. A cyclic voltammogram (CV) of $[Cu(phendione)_2]^{2+}$ was obtained in degassed Tris buffer (10 mM Tris, 100 mM KCl, 2.5 mM $MgCl_2$, 1 mM $CaCl_2$, pH 7.6) at a glassy carbon working electrode. CV was performed with a scan rate of 0.1 V/s against an AgCl/Ag reference electrode with a Pt counter electrode.

Formation of DNA Monolayers with Activation from Primary or Secondary Electrodes

To prepare DNA-modified surfaces for biomolecule detection assays, alkyne-labeled duplex DNA is attached to mixed thiol monolayers containing 50% azide and 50% phosphate head groups through electrochemically-activated click chemistry. An overview of the process of electrochemical click to attach DNA to an electrode, followed by DNA CT-facilitated current measurement, is shown in Figure 5.3. Based on previous studies, a 1:1 ratio of azide to phosphate head groups provides adequate spacing between the individual helices for substrate access, while maintaining a sufficient concentration of DNA on the surface for reliable detection.[20] Importantly, electrochemical titrations of methylene blue and ferricyanide individually, as well as mixtures of both methylene blue and ferricyanide together, established that these alkylthiol mixed monolayers remain effectively passivated to solutions of up to 8 μM methylene blue and 500 μM ferricyanide, showing no electrochemical signal at these concentrations (data not shown).

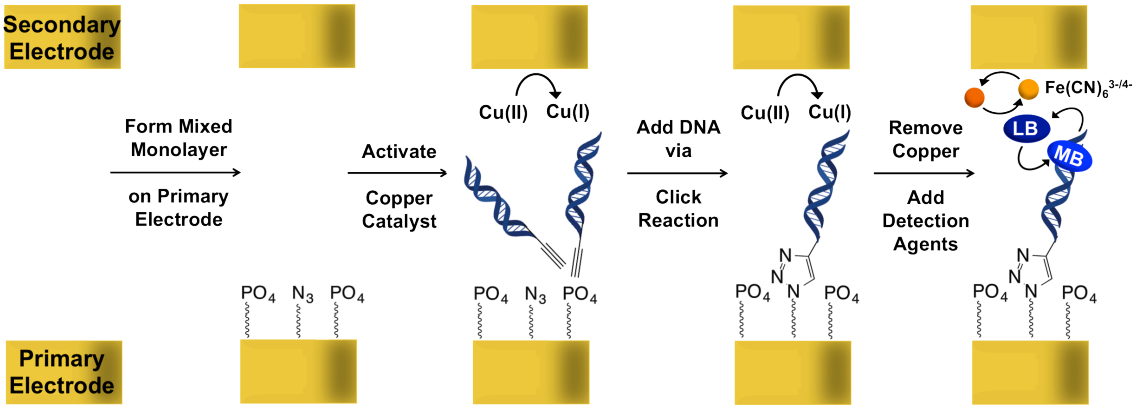

Figure 5.3 General strategy for monolayer formation and detection. First, a mixed alkanethiol monolayer is formed on the primary electrode array containing phosphate and azide head groups. Subsequently, a copper catalyst for click chemistry is activated at the secondary electrode to enable the click reaction to proceed between the surface-bound azides and alkyne-modified DNA. Finally, all copper is removed, and methylene blue and ferricyanide are added for electrochemical detection.

Solutions of $[Cu(phendione)_2]^{2+}$ (typically 1 mM) are used for the inert catalytic precursor; activation to Cu(I) is accomplished by applying a constant potential of -350 mV (vs. AgCl/Ag) to a secondary electrode for 15 minutes. As can be seen from the CVs in Figure 5.4, after copper activation and subsequent rinsing of the surface, no residual copper is evident on the surface.

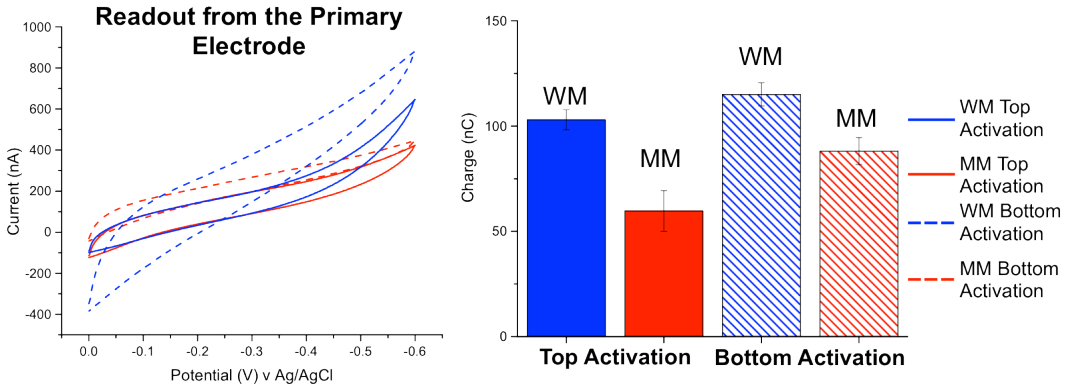

Figure 5.4 Effects of catalyst activation at the primary as compared to the secondary working electrodes with conventional detection from the DNA-modified electrode. (*Left*) Cyclic voltammetry (ν = 100 mV/s) of 4 μM MB / 300 μM $[K]_3[Fe(CN)_6]$ in Tris buffer, using the two-electrode multiplexed platform with a 127-μm spacer separating the primary- and secondary-electrode arrays. Data were recorded at four separate primary electrodes featuring an underlying 50/50 azide/phosphate monolayer, covalently modified with either well-matched (blue) or mismatched (red) alkyne-labeled DNA duplexes (18-mers). The solid traces were obtained at electrodes prepared by $Cu(phendione)_2^{2+}$ activation at the corresponding secondary electrodes, while the dashed traces were obtained by activating $Cu(phendione)_2^{2+}$ directly at the primary electrodes. (*Right*) Charges obtained by integrating the cyclic voltammograms. Electrodes prepared by catalyst activation at the secondary electrode display modest, though significantly better mismatch discrimination.

Cyclic voltammetry (CV) from the primary, DNA-modified electrode (DME) is a standard technique for electrochemical analysis of DNA CT through monolayers. Thus, CVs of DNA monolayers formed by catalyst activation at either the primary or the secondary electrode were acquired to evaluate monolayer characteristics. The CVs do not have the conventional redox couple from methylene blue on DMEs because of both the low coverage of DNA and the concentrations of the redox probe and electron sink required for detection at the secondary electrode. The CVs in Figure 5.4 also highlight complications arising from copper activation at the primary electrode; the details of mismatch analysis are described below. Most notably, background currents are larger at DNA-modified surfaces formed by activation at the primary electrode (primary electrode activation) versus the secondary electrode, likely due to a layer of copper precipitate on the DNA monolayer. This precipitate is only observable on the electrode used for catalyst activation. If the primary electrode is used for activation, copper precipitates on the DNA monolayer. Conversely, if the secondary electrode is used for activation, the copper precipitate occurs at that bare electrode surface and is easily removed by polishing the array prior to detection with this array. Copper activation at the primary electrode further yields surfaces that exhibit variable capacitances between well matched and mismatched DNA monolayers, indicating non-equivalent monolayer formation. The CVs from substrate electrodes patterned by a secondary electrode, in contrast, have consistent capacitance. Nevertheless, the difference in charge measured by well-matched DNA as compared to mismatched DNA, a hallmark of DNA CT, remains only moderate when these monolayers are measured from the primary electrode.

Electrochemical impedance spectroscopy (EIS)[36] was also performed to evaluate the effect of copper-film deposition on the electrochemical properties of DNA monolayers formed *via* $[Cu(phendione)_2]^{2+}$ reduction at either the primary or secondary electrode, as well as at bare gold electrodes and electrodes modified with only the underlying mixed alkylthiol monolayers. EIS was executed using ferricyanide and ferrocyanide, a standard method of label-free DNA detection, which is based on the amount of access the small molecule has to the electrode surface.[36, 37] Nyquist plots (Figure 5.5) constructed from data collected at these latter two surfaces display a small impedance arc, consistent with low surface capacitance and a response dominated mainly by diffusion of the small molecule to the surface.[36, 38-40] In contrast, the presence of DNA on the electrode surface partially blocks ferricyanide from interacting with the electrode, resulting in a significantly larger capacitive arc. Consistent with the CV data, the Nyquist plot from a DNA monolayer formed *via* catalyst activation from the substrate electrode shows a substantially larger (and less reproducible) arc, indicating higher electron-transfer resistance than that of the analogous DNA film prepared *via* activation from the secondary electrode. Presumably, deposition of copper-containing species following electrochemical reduction of $[Cu(phendione)_2]^{2+}$ further passivates the now heterogeneous surface from analytes in solution.

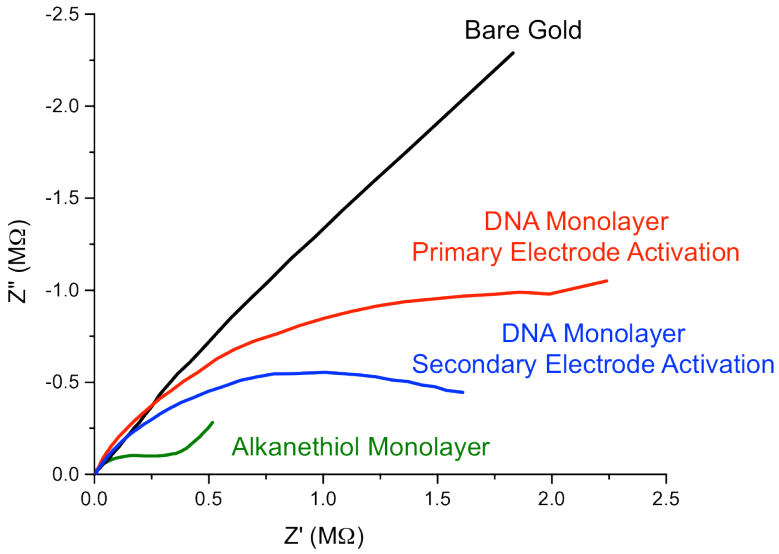

Figure 5.5 Nyquist plots of electrochemical impedance spectroscopy of differentially formed monolayers. Shown are results for a bare gold electrode (black), a mixed monolayer of azide and phosphate-terminated thiols (green), a DNA monolayer formed from $[Cu(phendione)_2]^{2+}$ catalyst activation from the secondary electrode (blue), and a DNA monolayer formed from the catalyst activation at the primary, substrate electrode (red). Conditions used for impedance spectroscopy were 400 μM ferrocyanide in phosphate buffer (5 mM phosphate, 50 mM NaCl, pH 7.0).

Electrochemical Readout at the Secondary versus Primary Electrode

To increase the sensitivity of DNA CT assays, we typically employ an electrocatalytic cycle using methylene blue (MB) and ferricyanide (Figure 5.1, 5.2).[12] Intercalated MB is reduced *via* DNA CT to leucomethylene blue (LB), which has a decreased affinity for DNA. Upon entering solution, the LB reduces freely diffusing ferricyanide to ferrocyanide, regenerating MB that re-intercalates into the film to begin the cycle again.

With a one working electrode system, the signal amplification afforded by the addition of the electron sink ferricyanide is limited to one turnover per ferricyanide molecule[39] Once ferricyanide is reduced to ferrocyanide in the vicinity of DNA monolayer, the effective concentration of electron sink at that location is very low, decreasing the signal amplification. In contrast, with a two working electrode system in which the electrodes are very close to one another, the effective concentration of ferricyanide is not depleted, as it is constantly replenished by the turnover of ferrocyanide at the secondary electrode. This ferrocyanide turnover enables more rounds of methylene blue turnover in a given amount of time with the two working electrode platform.

In fact, the incorporation of a secondary electrode enables the system to function as a collector-generator. The secondary electrode is held at a sufficiently positive potential to oxidize the ferrocyanide that is generated in solution as a result of the reduction of ferricyanide by LB following DNA CT. When the primary and secondary electrodes are sufficiently close, the current generated from the oxidation of ferrocyanide at the secondary electrode provides a significantly more amplified electrochemical signal than can be achieved in a one electrode system; the secondary electrode enables more

rounds of turnover in a given period of time than electrocatalysis with the primary electrode alone. If ferricyanide is reduced in solution by LB due to DNA-mediated reduction of MB, more ferrocyanide is present at the secondary electrode, where it is reoxidized to generate a large current at that electrode. In contrast, if no DNA CT occurs at the primary electrode, no current is generated at the secondary electrode, negating the need for background correction. Our platform can function as a collector-generator when starting with either ferrocyanide, as with conventional collector-generators, or ferricyanide, which is converted to ferrocyanide following DNA CT.

For this platform to effectively function as a collector-generator, the distance between the two sets of electrodes must be sufficiently close to ensure that the local concentration of ferricyanide is not depleted, while maintaining sufficient distance to obtain DNA-mediated signals. With scanning electrochemical microscopy (SECM), the optimal distance between the tip and the electrode surface is determined by an approach curve.[41, 42] We have similarly optimized the distance between our two working electrodes by varying the height of the Teflon spacer between the two arrays, with heights ranging from 50 μm to 1500 μm (Figure 5.6). Using ferricyanide and MB, the current as well as signal decrease upon incorporation of a single-base mismatch are measured.

Based on the currents obtained with the variation of spacer height, it may be the case that if the spacer is too close to the surface, our signals are no longer DNA-mediated. This is likely what is occurring with the 50 μm spacer, with which we do not see mismatch discrimination. The spacer that provides large currents while maintaining

DNA-mediated CT, as confirmed by mismatch discrimination, is the 127 μm spacer, which was therefore used for all experiments.

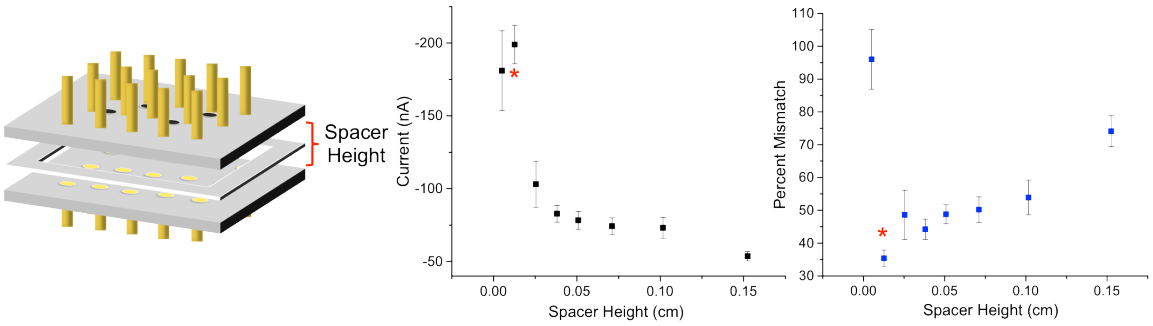

Figure 5.6 Optimizing the spacer height. Eight Teflon spacers of different heights were tested for electrochemical signal and mismatch discrimination. The spacer between the two electrode arrays establishes the gap between the two electrodes (left). The current from constant current amperometry obtained as a function of spacer height (center) is maximized with the 127 µm spacer (red asterisk). Mismatch discrimination as a function of spacer height (right) is reported as a ratio of the mismatched signal to the well matched signal, with maximal discrimination also observed with the 127 µm spacer (red asterisk). All electrochemistry was conducted in Tris buffer (10 mM Tris, 100 mM KCl, 2.5 mM $MgCl_2$, 1 mM $CaCl_2$, pH 7.6) with 4 µM methylene blue and 300 µM $K_3[Fe(CN)_6]$. 18-mer well matched and mismatched DNA was used.

As illustrated in Figure 5.7, we have also confirmed that our system functions as a collector-generator with both ferrocyanide and ferricyanide, which is important to ensure that time-resolved changes to the system are sensitively monitored.[41, 42] To test the collector-generator capabilities of the platform, generally the current at the secondary electrode is constantly monitored with an applied positive potential. Preliminarily, no potential is applied to the primary. After 15 seconds, a negative potential is applied to the DME. This causes a large amount of current to be immediately generated at the secondary electrode by electrocatalysis at the primary electrode. This initial burst of current, due to the rapid dissociation of a large amount of methylene blue that was intercalated into the DNA, depletes to a steady-state current as a cycle is established (Figure 5.7). When the secondary electrode is held at a positive, oxidizing potential and ferricyanide is used (Figure 5.7a), no current is evident before the potential is applied to the primary electrode. When ferrocyanide is monitored without a potential applied to the primary electrode, a small current is observed at the secondary electrode due to the preliminary oxidation of ferrocyanide to ferricyanide (Figure 5.7b). However, this small current quickly decreases as the ferrocyanide is depleted in the absence of DNA CT at the primary electrode. Once a potential is applied to the primary electrode with either ferricyanide or ferrocyanide, current is generated. This behavior mimics characteristic behavior of SECM substrates modified with a conductive film,[43-47] indicating that the DNA film on the primary electrode is conductive (due to DNA CT) and is responsible for the current output at the secondary electrode.

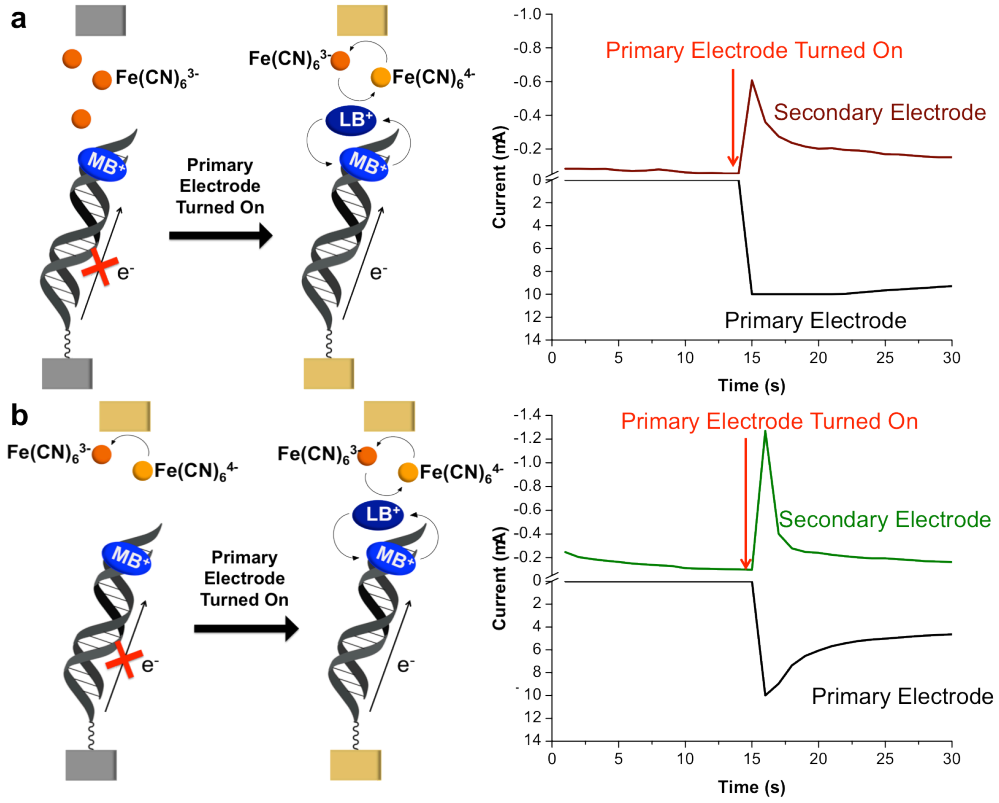

Figure 5.7 Detection strategy (*left*) and constant-potential amperometry assay (*right*) for DNA CT using the two-electrode detection platform. Electrochemical readout is carried out at a single, addressable electrode in the secondary array held at +0.35 V. In (**a**), the thin layer between the primary and secondary electrode arrays contains 4 μM MB and 300 μM $Fe(CN)_6^{3-}$. Because the applied potential is positive of the $Fe(CN)_6^{3-/4-}$ redox couple, there is no initial current (shown in red) at the secondary electrode. 15 seconds into the experiment, the entire primary electrode array (current shown in black) is activated at a potential of -0.40 V. This initiates the MB/$Fe(CN)_6^{3-}$ electrocatalytic cycle, and current begins to flow at the secondary electrode due to the re-oxidation of $Fe(CN)_6^{4-}$ generated at the primary array. For sensing applications, readout at the secondary electrode is measured only after a steady-state current is achieved (~ 30 s) to eliminate any complications arising from double-layer charging effects. The lower panel (**b**) shows the analogous experiment, except that the thin-layer solution initially contains 4 μM MB and 300 μM $Fe(CN)_6^{4-}$. When the secondary electrode is turned on at time zero, there is an initial current (shown in green) due to the oxidation of $Fe(CN)_6^{4-}$ to $Fe(CN)_6^{3-}$. This current rapidly approaches zero as the $Fe(CN)_6^{4-}$ is converted to $Fe(CN)_6^{3-}$ within the thin layer. At the 15-s mark, the primary array is turned on, and the assay proceeds as in (**a**).

Single-Base Mismatch Detection with Non-covalent and Covalent Redox Probes

The collector-generator experiment provides evidence that our DNA films are conductive, consistent with DNA CT processes. However, the key experiment demonstrating that this electrochemical process is mediated by transport through the DNA helix is electrochemical signal attenuation upon incorporation of a single-base mismatch. Single-base mismatch discrimination was previously discussed in the context of catalyst activation with detection at the primary electrode and spacer height. Additionally, evaluation of mismatches in DNA monolayers with detection at the secondary electrode was also tested with catalyst activation at both the primary and secondary electrodes. For this analysis, well matched and mismatched DNA monolayers were formed and evaluated side-by-side on the same electrode array with copper catalyst activation at either the primary or secondary electrode. Electrochemical responses were measured by constant potential amperometry with 4 μM MB and 300 μM ferricyanide for a time previously optimized to reach a steady-state current, 90 s.[33]

When constant potential amperometry is conducted from the secondary electrode, the advantages of both catalyst activation and electrochemical readout from this electrode are evident. The difference in current between well-matched and mismatched signals is large, and the current readout is very robust for monolayers formed by copper activation from a secondary electrode (Figure 5.8). In contrast, when monolayers are formed by copper activation from the primary electrode, the current is small, and mismatch discrimination is poor. The differences observed in signal size, consistency, and mismatch discrimination highlight the importance of catalyst activation from the secondary electrode. Furthermore, large signal differences obtained from secondary

electrode readout obviate the need for dramatic background subtractions, essentially providing an on/off sensor for mismatch detection.

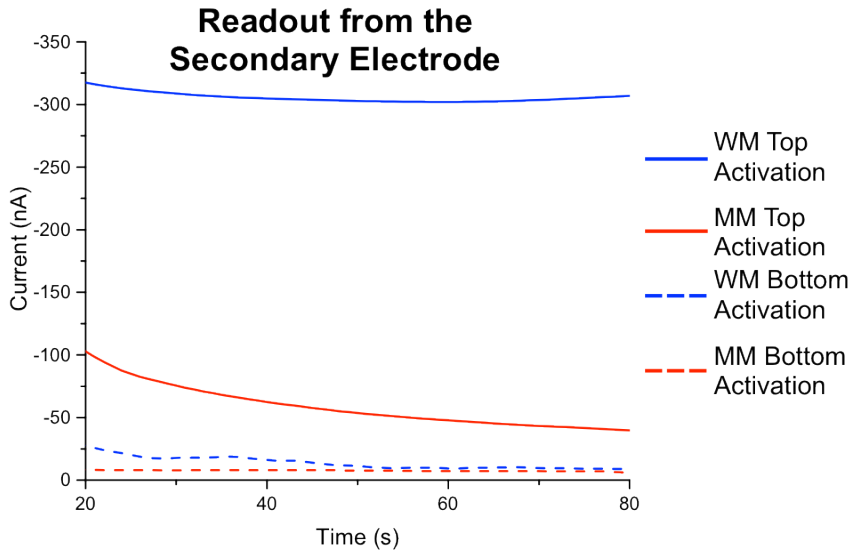

Figure 5.8 Mismatch detection with electrochemical readout at the secondary electrode. Constant-potential amperometry was conducted at the secondary electrodes with an applied potential of +0.35 V, while the primary-electrodes were held at -0.40 V in the presence of 4 μM MB and 300 μM $Fe(CN)_6^{3-}$. The blue traces represent currents measured at readout electrodes complementary to well-matched DNA sequences (18-mers) on the primary array, while the red traces represent the analogous currents generated at electrodes complementary to mismatched duplexes. For comparison (dashed lines), the identical assay was carried out on a separate array in which the DNA duplexes were conjugated *via* copper(II) activation directly at the primary electrodes; clearly, greater signal differential between well- *vs,* mismatched sequences occurs when monolayers are formed by catalyst activation at the secondary electrode. In these experiments, all primary-array electrodes were first modified with an underlying 50/50 azide/phosphate monolayer before DNA conjugation.

Additionally, we have investigated detection on this platform with a covalent redox probe, which may be favorable for some biomolecule detection applications. Nile Blue, a covalent reporter that is electronically conjugated to the DNA π-stack through the linker,[34] was found to successfully participate in electrocatalytic turnover, resulting in significant mismatch discrimination despite being covalently tethered to DNA (Figure 5.9). A 60±10% decrease in the current upon incorporation of a single base mismatch occurs with the covalent Nile blue redox probe, as compared to an 80±10% decrease with noncovalent methylene blue. This difference in mismatch discrimination is likely due to the fact that noncovalent methylene blue is not limited to one association per DNA, nor is it conformationally or spatially constrained as is the covalent Nile Blue. It is therefore unsurprising that MB yields larger signals and larger differential. This result is consistent with previous electrocatalytic mismatch discrimination, in which larger differentials are observed with free probes than with covalent probes.

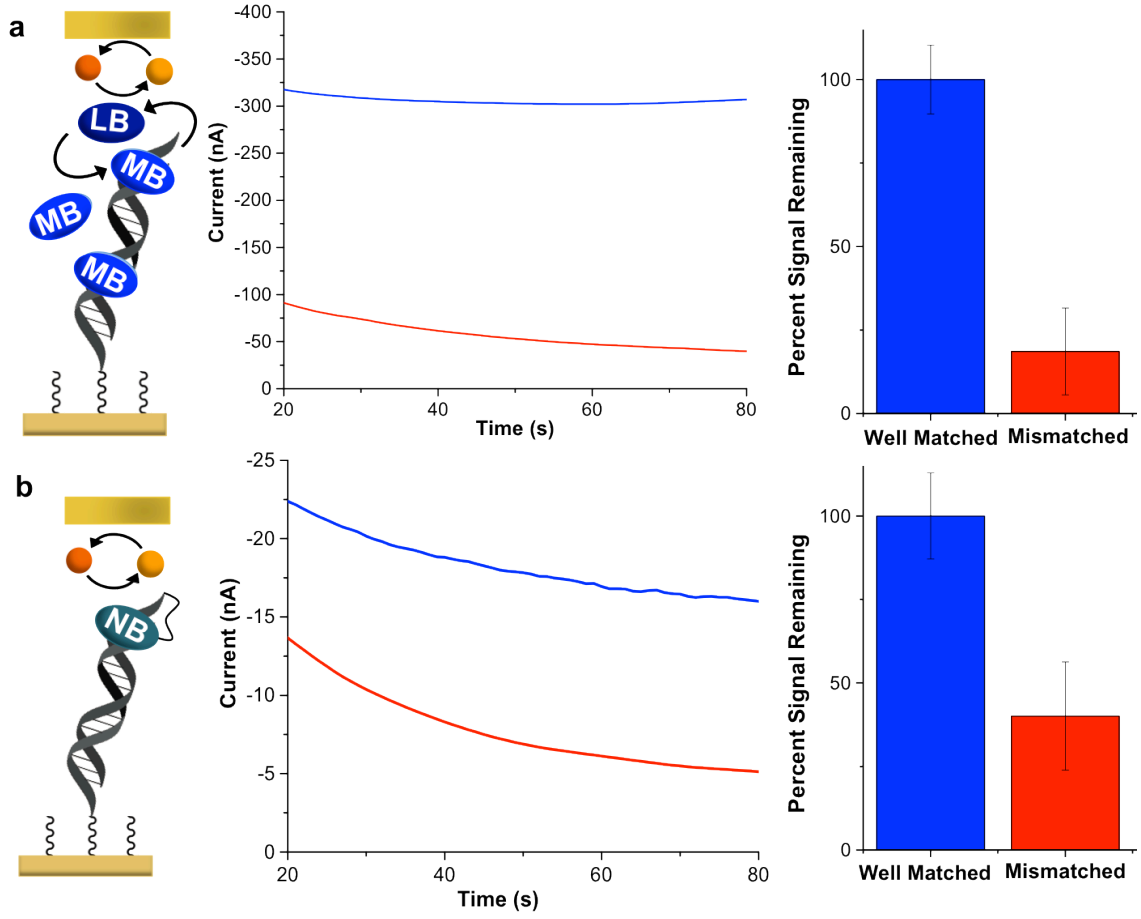

Figure 5.9 Comparison of mismatch discrimination recorded with the two-electrode platform using methylene blue *vs.* Nile blue redox reporters. (**a**) Electrochemical readout recorded at a secondary electrode during the electrocatalytic reduction of 400 μM $Fe(CN)_6^{3-}$ in the presence of 4 μM MB at primary electrodes modified with well-matched DNA duplexes (blue), and mismatched DNA duplexes (red). (**b**) The same assay, but with Nile blue covalently bound to the DNA probe sequences substituting for MB. Percent signal changes were calculated from the amperometry data recorded 90 seconds after initiation of the electrochemical readout.

Detection of DNA-binding Proteins

To establish the relevance of this platform for biomolecule detection, DNA-binding protein detection was also investigated with two transcription factors, TBP and CopG. Both bind to specific sequences of DNA, kink the duplex to a large degree, and are therefore capable of attenuating CT. The transcription factor TBP, TATA-binding protein, a subunit of the eukaryotic TFIID transcription factor, was previously employed as a measure of sensitivity for a DNA CT-based protein detection platform.[34, 48] This protein kinks DNA by over 80° when bound to its TATA target sequence with a K_D of 3.3 nM,[49] destacking the DNA bases and attenuating DNA CT.[20] Detection limits in the concentration range of the K_D support that a platform is sufficiently sensitive to detect protein binding. In the past, we have utilized covalent redox probes for protein detection, but the ease of detection with our two-electrode platform allows simple discrimination with non-covalent MB.

The multiplexed nature of our platform further enables the specific detection of multiple proteins simultaneously.We therefore additionally investigated the detection of the transcription repressor CopG, which binds DNA as a tetramer at an ACGTxxxxxACGT site, bending the helix up to 120°, with a nM binding affinity.[50-52] Each of these proteins was individually titrated onto monolayers to determine detection limits. Subsequently, specific detection of these proteins on the same multiplexed array was performed.

The titrations (Figure 5.10) indicate significant signal decreases, greater than 30%, associated with binding of both proteins at very low concentrations (10 nM), which, based on our extremely small volumes, translates to less than 50 femtomoles of protein.

From these titration curves, dissociation constants can be calculated for both proteins on our DMEs using a cooperative binding model (Hill model).[20] TBP has a surface K_D of 14±2 nM, and CopG has a surface K_D of 17±4 nM. Both TBP and CopG are therefore detectable at concentrations near their solution K_D's (3.3 nM and 10 nM, respectively).

We additionally specifically and selectively detected both of these proteins on the same multiplexed array. Each transcription factor was added to the array modified with three electrodes containing a non-binding sequence, six electrodes modified with DNA containing a TBP binding site, and six electrodes modified with DNA containing a CopG binding site. In this assay, one protein (either TBP or CopG) is added to the surface. Signal attenuation is then measured and compared to the non-binding sequence (the positive control). The surface is subsequently rinsed, and the second protein is added with measurement of the signal attenuation. In all cases, signal attenuation is only observed at DNA containing the binding sequence of the protein added, verifying changes are only due to the specific binding of a particular protein. Greater variability between protein detection experiments is observed in the dual protein detection experiments, as compared to the individual titrations, likely because of the added normalization of these data to a non-binding positive control sequence. This additional normalization is necessary for combined protein experiments to confirm that signal decreases are due to specific binding of one of the proteins.

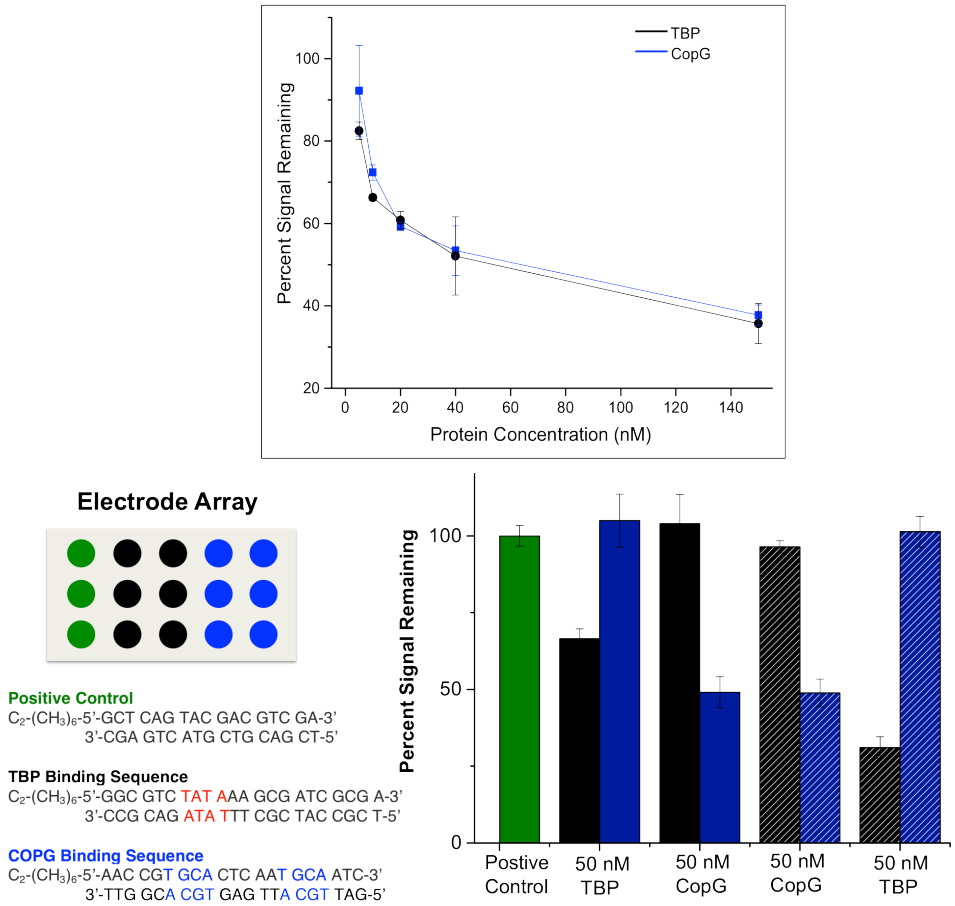

Figure 5.10 Titration of transcription factors TATA-binding protein (TBP) and CopG on two-electrode array. Each protein was titrated onto an array in concentrations ranging from 0 nM to 150 nM. Shown (top) is the percent electrochemical signal remaining from constant potential amperometry plotted as a function of protein concentration. The proteins caused significant signal decreases on the arrays in very low nanomolar concentrations. All electrochemistry was conducted in Tris buffer (10 mM Tris, 100 mM KCl, 2.5 mM $MgCl_2$, 1 mM $CaCl_2$, pH 7.6) with 4 μM methylene blue and 300 μM $K_3[Fe(CN)_6]$. Constant potential amperometry at the secondary electrode was conducted with an applied potential of 350 mV v. AgCl/Ag to the secondary electrode and -400 mV v. AgCl/Ag to the primary electrode for 90 seconds. Specific detection of transcription factors TBP and CopG on a single array is also shown (bottom right). Arrays are formed with six electrodes modified with DNA containing specific binding sites for each of the transcription factors TBP and CopG, as well as three electrodes containing positive control DNA that does not contain the binding site for either protein. A single protein was added to the surface at a 50 nM concentration, and the signal decrease for each sequence was monitored. The second protein was subsequently added, and signal decreases monitored. TBP detection followed by CopG detection is shown with solid bars, while CopG detection followed by TBP detection is shown with dashed bars. The

TBP binding sequence is represented by black, both in terms of the location of the electrodes modified with this sequence on the electrode array (bottom left, black circles) and in terms of the percent signal remaining for this sequence (bottom right, black bars). Independent of which protein was added first, signal decreases were only observed on the sequences to which the specific protein binds.

Implications

Although the copper(I)-catalyzed Huisgen cycloaddition[21] is attractive for biomolecule modification because of its bioorthogonality, issues with this reaction for DNA-based applications arise due to the instability of copper(I) complexes in aqueous solutions as well as their potential reactivity with DNA. One strategy to mitigate these complications is to generate Cu(I) *in situ* through electrochemical reduction of a more inert Cu(II) complex, although complications with this method may still arise (Figures 5.2, 5.4 and 5.8). These difficulties are easily surmounted, though, through the electrochemical activation of $[Cu(phendione)_2]^{2+}$ from a secondary working electrode, which minimizes the interference of degraded catalyst with the DNA film, as the copper precipitates on the bare, secondary electrode. Any catalyst precipitate on the secondary electrode array is easily removed through polishing prior to application of this array for detection.

In addition to enabling the formation of superior DNA monolayers, the second working electrode facilitates sensitive detection without the need for background corrections. In contrast to electrocatalytic signal amplification detected at the DME, in which amplification is limited by depletion of the local concentration of ferricyanide, a secondary electrode sufficiently close to the DME removes the dependence of the signal amplification on the diffusion of additional ferricyanide. As we demonstrate, this platform (Figures 5.1, 5.2) behaves as a collector-generator with either ferricyanide or ferrocyanide (Figure 5.7). Furthermore, large background corrections are unnecessary, as current only flows from the primary to the secondary electrode when a redox probe is reduced by DNA CT, and the current generated at the secondary electrode is wholly

dependent on the amount of DNA CT occurring at the primary electrode surface. Our signals were also confirmed to be DNA mediated through the detection of a single-base mismatch. Both covalent (Nile blue) and noncovalent (methylene blue) redox probes coupled to electrocatalytic signal amplification yielded significant signal attenuation upon incorporation of a single-base mismatch when probed from the secondary electrode by constant potential amperometry (Figures 5.8, 5.9).

For any nucleic acid platform, monitoring protein binding is an especially difficult challenge due to the required sensitivity and specificity, as well as the often-small signal differentials associated with binding. DNA CT-based platforms offer a unique opportunity for such detection, as proteins that destack DNA bases upon binding yield significant decreases in electrochemical signals. However, there is no guarantee that such detection is translatable to a two working electrode platform. In fact, we observe that this platform does enable the determination of sensitive and specific protein binding, both of a previously reported transcription factor, TBP, and a similar transcription factor, CopG, whose binding had not been previously evaluated by DNA CT. Indeed, we successfully detect femtomoles of both proteins at concentrations near their dissociation constants sequence-specifically.

The Two-Working Electrode Platform

Here, we have described an especially sensitive multiplexed, two working electrode platform for DNA CT-based electrochemical detection. This platform enables low density DNA monolayer formation and amplified electrochemical readout through the incorporation of a second working electrode. Catalyst activation at a secondary

electrode is essential to maintain the integrity of the DNA, as shown by EIS, CV, and constant potential amperometry. Detection from the secondary electrode is similarly necessary to provide high sensitivity without large background signals. These signals have further been confirmed to be DNA mediated by mismatch discrimination experiments. Importantly, this platform is capable of specifically detecting femtomoles of the transcription factors, TBP and CopG. This multiplexed, two-electrode detection platform thus broadens the scope and applications for detection using DNA CT.

References

1. Das, J., Cederquist, K. B., Zaragoza, A. A., Lee, P. E., Sargent, E. H., and Kelley, S. O. (2012) An ultrasensitive universal detector based on neutralizer displacement, *Nat. Chem. 4*, 642-648.

2. Gooding, J. J. (2002) Electrochemical DNA Hybridization Biosensors, *Electroanalysis 14*, 1149-1156.

3. Kelley, S. O., Mirkin, C. A., Walt, D. R., Ismagilov, R. F., Toner, M., and Sargent, E. H. (2014) Advancing the speed, sensitivity and accuracy of biomolecular detection using multi-length-scale engineering, *Nat. Nanotechnol. 9*, 969-980.

4. Lam, J. C. F., Aguirre, S., and Li, Y. (2010) Nucleic Acids as Detection Tools, In *The Chemical Biology of Nucleic Acids*, pp 401-431, John Wiley & Sons, Ltd.

5. Liu, J., Cao, Z., and Lu, Y. (2009) Functional nucleic acid sensors, *Chem. Rev. 109*, 1948-1998.

6. Pei, H., Lu, N., Wen, Y., Song, S., Liu, Y., Yan, H., and Fan, C. (2010) A DNA nanostructure-based biomolecular probe carrier platform for electrochemical biosensing, *Adv. Mater. 22*, 4754-4758.

7. Soleymani, L., Fang, Z., Sun, X., Yang, H., Taft, B. J., Sargent, E. H., and Kelley, S. O. (2009) Nanostructuring of patterned microelectrodes to enhance the sensitivity of electrochemical nucleic acids detection, *Angew. Chem. Int. Ed. 48*, 8457-8460.

8. Wang, J. (2002) Electrochemical nucleic acid biosensors, *Anal. Chim. Acta 469*, 63-71.

9. Yang, H., Hui, A., Pampalakis, G., Soleymani, L., Liu, F. F., Sargent, E. H., and Kelley, S. O. (2009) Direct, electronic microRNA detection for the rapid determination of differential expression profiles, *Angew. Chem. Int. Ed. 48*, 8461-8464.

10. Gorodetsky, A. A., Buzzeo, M. C., and Barton, J. K. (2008) DNA-mediated electrochemistry, *Bioconjug. Chem. 19*, 2285-2296.

11. Drummond, T. G., Hill, M. G., and Barton, J. K. (2003) Electrochemical DNA sensors, *Nat. Biotechnol. 21*, 1192-1199.

12. Furst, A., Hill, M. G., and Barton, J. K. (2014) Electrocatalysis in DNA Sensors, *Polyhedron 84*, 150-159.

13. Muren, N. B., Olmon, E. D., and Barton, J. K. (2012) Solution, surface, and single molecule platforms for the study of DNA-mediated charge transport, *Phys. Chem. Chem. Phys. 14*, 13754-13771.

14. Abi, A., and Ferapontova, E. E. (2012) Unmediated by DNA electron transfer in redox-labeled DNA duplexes end-tethered to gold electrodes, *J. Am. Chem. Soc. 134*, 14499-14507.

15. Kelley, S. O., Jackson, N. M., Hill, M. G., and Barton, J. K. (1999) Long-Range Electron Transfer through DNA Films, *Angew. Chem. Int. Ed. 38*, 941-945.

16. Levicky, R., Herne, T. M., Tarlov, M. J., and Satija, S. K. (1998) Using Self-Assembly To Control the Structure of DNA Monolayers on Gold: A Neutron Reflectivity Study, *J. Am. Chem. Soc. 120*, 9787-9792.

17. Murphy, J. N., Cheng, A. K., Yu, H. Z., and Bizzotto, D. (2009) On the nature of DNA self-assembled monolayers on Au: measuring surface heterogeneity with electrochemical in situ fluorescence microscopy, *J. Am. Chem. Soc. 131*, 4042-4050.

18. Ricci, F., Lai, R. Y., Heeger, A. J., Plaxco, K. W., and Sumner, J. J. (2007) Effect of molecular crowding on the response of an electrochemical DNA sensor, *Langmuir 23*, 6827-6834.

19. Sam, M., Boon, E. M., Barton, J. K., Hill, M. G., and Spain, E. M. (2001) Morphology of 15-mer duplexes tethered to Au(111) probed using scanning probe microscopy, *Langmuir 17*, 5727-5730.

20. Furst, A. L., Hill, M. G., and Barton, J. K. (2013) DNA-modified electrodes fabricated using copper-free click chemistry for enhanced protein detection, *Langmuir 29*, 16141-16149.

21. Huisgen, R., Grashey, R., and Sauer, J. (2010) Cycloaddition reactions of alkenes, In *The Alkenes (1964)*, pp 739-953, John Wiley & Sons, Ltd.

22. Collman, J. P., Devaraj, N. K., and Chidsey, C. E. (2004) "Clicking" functionality onto electrode surfaces, *Langmuir 20*, 1051-1053.

23. Gerasimov, J. Y., and Lai, R. Y. (2011) Design and characterization of an electrochemical peptide-based sensor fabricated via"click" chemistry, *Chem. Commun. 47*, 8688-8690.

24. Kazakov, S. A., Astashkina, T. G., Mamaev, S. V., and Vlassov, V. V. (1988) Site-specific cleavage of single-stranded DNAs at unique sites by a copper-dependent redox reaction, *Nature 335*, 186-188.

25. Meijler, M. M., Zelenko, O., and Sigman, D. S. (1997) Chemical Mechanism of DNA Scission by (1,10-Phenanthroline)copper. Carbonyl Oxygen of 5-Methylenefuranone Is Derived from Water, *J. Am. Chem. Soc. 119*, 1135-1136.

26. Shuman, M. S., and Woodward, G. P. (1977) Stability constants of copper-organic chelates in aquatic samples, *Environmental Science & Technology 11*, 809-813.

27. Canete, S. J., and Lai, R. Y. (2010) Fabrication of an electrochemical DNA sensor array via potential-assisted "click" chemistry, *Chem. Commun. 46*, 3941-3943.

28. Devaraj, N. K., Dinolfo, P. H., Chidsey, C. E., and Collman, J. P. (2006) Selective functionalization of independently addressed microelectrodes by electrochemical activation and deactivation of a coupling catalyst, *J. Am. Chem. Soc. 128*, 1794-1795.

29. Devaraj, N. K., Miller, G. P., Ebina, W., Kakaradov, B., Collman, J. P., Kool, E. T., and Chidsey, C. E. (2005) Chemoselective covalent coupling of oligonucleotide probes to self-assembled monolayers, *J. Am. Chem. Soc. 127*, 8600-8601.

30. Ripert, M., Farre, C., and Chaix, C. (2013) Selective functionalization of Au electrodes by electrochemical activation of the "click" reaction catalyst, *Electrochimica Acta 91*, 82-89.

31. Furst, A., Landefeld, S., Hill, M. G., and Barton, J. K. (2013) Electrochemical patterning and detection of DNA arrays on a two-electrode platform, *J. Am. Chem. Soc. 135*, 19099-19102.

32. Quinton, D., Maringa, A., Griveau, S., Tebello, N., and Bedioui, F. (2013) Surface patterning using scanning electrochemical microscopy to locally trigger a "click" chemistry reaction, *Electrochem. Commun. 31*, 112-115.

33. Furst, A. L., Muren, N. B., Hill, M. G., and Barton, J. K. (2014) Label-free electrochemical detection of human methyltransferase from tumors, *Proc. Natl. Acad. Sci. USA 111*, 14985-14989.

34. Gorodetsky, A. A., Ebrahim, A., and Barton, J. K. (2008) Electrical detection of TATA binding protein at DNA-modified microelectrodes, *J. Am. Chem. Soc. 130*, 2924-2925.

35. Hong, V., Presolski, S. I., Ma, C., and Finn, M. G. (2009) Analysis and optimization of copper-catalyzed azide-alkyne cycloaddition for bioconjugation, *Angew. Chem. Int. Ed. 48*, 9879-9883.

36. Ceres, D. M., Udit, A. K., Hill, H. D., Hill, M. G., and Barton, J. K. (2007) Differential ionic permeation of DNA-modified electrodes, *J. Phys. Chem. B 111*, 663-668.

37. Janek, R. P., Fawcett, W. R., and Ulman, A. (1998) Impedance spectroscopy of self-assembled monolayers on Au(111): Sodium ferrocyanide charge transfer at modified electrodes, *Langmuir 14*, 3011-3018.

38. Bard, A., and Faulkner, L. (2001) *Electrochemical Methods: Fundamentals and Applications*, John Wiley & Sons, Inc.

39. Boon, E. M., Barton, J. K., Bhagat, V., Nersissian, M., Wang, W., and Hill, M. G. (2003) Reduction of Ferricyanide by Methylene Blue at a DNA-Modified Rotating-Disk Electrode, *Langmuir 19*, 9255-9259.

40. Kafka, J., Pänke, O., Abendroth, B., and Lisdat, F. (2008) A label-free DNA sensor based on impedance spectroscopy, *Electrochimica Acta 53*, 7467-7474.

41. Fernandez, J. L., and Bard, A. J. (2003) Scanning electrochemical microscopy. 47. Imaging electrocatalytic activity for oxygen reduction in an acidic medium by the tip generation-substrate collection mode, *Anal. Chem. 75*, 2967-2974.

42. Martin, R. D., and Unwin, P. R. (1998) Theory and Experiment for the Substrate Generation/Tip Collection Mode of the Scanning Electrochemical Microscope:â€‰ Application as an Approach for Measuring the Diffusion Coefficient Ratio of a Redox Couple, *Anal. Chem. 70*, 276-284.

43. Liu, B., Bard, A. J., Li, C. Z., and Kraatz, H. B. (2005) Scanning electrochemical microscopy. 51. Studies of self-assembled monolayers of DNA in the absence and presence of metal ions, *J. Phys. Chem. B 109*, 5193-5198.

44. Turcu, F., Schulte, A., Hartwich, G., and Schuhmann, W. (2004) Label-free electrochemical recognition of DNA hybridization by means of modulation of the feedback current in SECM, *Angew. Chem. Int. Ed. 43*, 3482-3485.

45. Wain, A. J., and Zhou, F. (2008) Scanning electrochemical microscopy imaging of DNA microarrays using methylene blue as a redox-active intercalator, *Langmuir 24*, 5155-5160.

46. Whitworth, A. L., Mandler, D., and Unwin, P. R. (2005) Theory of scanning electrochemical microscopy (SECM) as a probe of surface conductivity, *Phys. Chem. Chem. Phys. 7*, 356-365.

47. Wierzbinski, E., Arndt, J., Hammond, W., and Slowinski, K. (2006) In situ electrochemical distance tunneling spectroscopy of ds-DNA molecules, *Langmuir 22*, 2426-2429.

48. Boon, E. M., Salas, J. E., and Barton, J. K. (2002) An electrical probe of protein-DNA interactions on DNA-modified surfaces, *Nat. Biotechnol. 20*, 282-286.

49. Hahn, S., Buratowski, S., Sharp, P. A., and Guarente, L. (1989) Yeast TATA-binding protein TFIID binds to TATA elements with both consensus and nonconsensus DNA sequences, *Proc. Natl. Acad. Sci. USA 86*, 5718-5722.

50. del Solar, G., Albericio, F., Eritja, R., and Espinosa, M. (1994) Chemical synthesis of a fully active transcriptional repressor protein, *Proc. Natl. Acad. Sci. USA 91*, 5178-5182.

51. del Solar, G. H., de al Campa, A. G., Perez-Martin, J., Choli, T., and Espinosa, M. (1989) Purification and characterization of RepA, a protein involved in the copy number control of plasmid pLS1, *Nucleic Acids Res. 17*, 2405-2420.

52. Gomis-Ruth, F. X., Sola, M., Acebo, P., Parraga, A., Guasch, A., Eritja, R., Gonzalez, A., Espinosa, M., del Solar, G., and Coll, M. (1998) The structure of plasmid-encoded transcriptional repressor CopG unliganded and bound to its operator, *EMBO J. 17*, 7404-7415.